Aviation Technology, Integration, and Operations Conference, 22-26 June 2015, Dallas, Texas

Comparison of CFD and Experimental Results of the LEAPTech Distributed Electric Propulsion Blown Wing

Alex M. Stoll*

Joby Aviation, Santa Cruz, California, 95060

The Leading Edge Asynchronous Propeller Technology (LEAPTech) demonstrator is a wing design for a four-place general aviation aircraft with high wing loading to reduce cruise drag and improve ride quality. Takeoff and landing performance is maintained by distributing 18 small propellers across the leading edge of the wing that blow the wing and increase the dynamic pressure during takeoff and landing. This configuration presented a complicated aerodynamic design problem because the relationship of design variables such as propeller tip speed and diameter to the realized blown wing performance (most importantly, lift) is difficult to accurately predict using low-order models such as momentum theory. Therefore, the design process involved the use of various higher-order aerodynamic simulation tools, particularly the STAR-CCM+ and FUN3D RANS codes and the VSPAERO vortex lattice code. The propellers are modeled with actuator disks, although the details of these actuator disk models differ. Experimental results were then obtained by constructing the wing at full scale, mounting it above a truck on a vibration-damping frame, and driving it along a runway at the design stall speed. A comparison of these experimental test results with computational results from these analysis tools is presented.

Nomenclature

C_L	lift coefficient
C_M	pitching moment coefficient
$C_{L_{\max}}$	maximum lift coefficient

Symbols

α	angle of attack

I. Introduction

An electric propulsion architecture, in which propellers are driven by electric motors, provides a different set of tradeoffs in aircraft design than a traditional propulsion architecture in which propellers driven by combustion engines. One possible application of such an electric propulsion architecture is embodied by the LEAPTech (Leading Edge Asynchronous Propeller Technology) concept, wherein a series of small propellers, each powered by a single electric motor, are distributed spanwise along the wing's leading edges. During takeoff and landing, these propellers are powered, and the axial induced velocity in the propeller downwash increases the dynamic pressure over the wing, allowing the use of a smaller wing to attain a given stall speed. This smaller wing incurs advantages of lower cruise drag (due to the lower wetted area) and improved ride quality.

This configuration, which has been described previously,[1] is the subject of an analytical and experimental study to verify predictions of the blown-wing aerodynamics. Most importantly, this study seeks to answer

*Aeronautical Engineer, 340 Woodpecker Ridge, AIAA Member.

whether such a distributed blown wing approach can obtain the lift forces required at the expected power levels and airspeeds. As such, this analysis is concentrated on the takeoff and landing segments of flight, where the greatest uncertainty lies. Many aspects of this aircraft configuration less important to the takeoff and landing performance, such as the fuselage, empennage, and cruise motors and propellers, are ignored in the current study.

II. Configuration Description

The wing design is relatively straightforward, to simplify construction and analysis. The center section, located where the fuselage would be in a full aircraft, is unswept, untapered, and untwisted; the remainder of the wing is of constant linear taper, sweep, and twist. The nacelles and propellers are all aligned such that their center axes make a 5° angle with the wing root, which is the intended orientation of the fuselage. (That is, the wing is imagined to be mounted to a fuselage at a 5° incidence angle.) At the tips, the wing terminates into an additional pair of nacelles, representative of the location of cruise motors and propellers on a full aircraft. Fowler flaps are deployed along the entire span between the wingtip nacelles and the root unswept section.

Eighteen brushless electric motors are mounted in nacelles regularly spaced spanwise along the wing leading edge and directly drive custom-designed propellers. The propellers spin at relatively low tip speeds to minimize noise. Propulsion in cruise flight is outside the scope of this analysis, but is intended to be performed by separate propellers mounted on the wingtips in such a configuration to significantly improve propulsive efficiency relative to traditional fuselage installations. In a full aircraft, the leading edge-mounted propellers are intended to fold flat against the respective nacelles during cruise to minimize drag.

Important parameters of this configuration are given in table 1, and a rendering of a potential flight demonstrator (a rewinged Tecnam P2006T) is shown in figure 1.

Figure 1. Rendering of a potential LEAPTech flight demonstrator

Planform area	55.2 ft^2	5.13 m^2
Reference chord	1.60 ft	0.487 m
Wingspan to wingtip nacelle centerline	31.0 ft	9.44 m
Aspect ratio	17.5	
Taper ratio	0.502	
Leading-edge sweep	10°	
Washout	4.0°	
Design stall speed (CAS)	61.0 knots	31.4 m/s
Design stall C_L at 3,000 lb	4.3	
Design takeoff power	300 hp	224 kW
Propeller diameter (each)	1.465 ft	0.447 m

Table 1. Design parameters

III. Computational Analysis

A. VLM: VSPAERO

Quick, lower-order analyses were performed with the vortex lattice code VSPAERO. The propellers are modeled as actuator disks; an inviscid elliptical loading model[2] prescribes the axial and radial velocities, and the swirl model employed accounts for viscous drag.[3] Although this method does not predict $C_{L_{\max}}$ well, it captures many aspects of the aerodynamics and aids in troubleshooting the higher-order methods.

B. RANS: STAR-CCM+

To achieve high confidence in the realizable aerodynamics of this configuration, extensive CFD analyses were performed. These were accomplished using the unstructured cell-centered finite-volume-based solver STAR-CCM+. Steady-state RANS simulations were performed, and turbulence closure was achieved using the SST k-ω model,[4,5] with transition modeled by the correlation-based γ-Re_θ[6,7] model. A limited number of cases instead employing the Spalart-Allmaras one-equation turbulence model[8] and limited to fully-turbulent flow were also analyzed and are denoted by "SA" when employing the standard Spalart-Allmaras model and "SA-RC" when employing rotation/curvature correction.[9]

To decrease the computational expense of these simulations, instead of resolving the full geometry of the propeller, the propellers are modeled by prescribing uniform volume force distributions over cylindrical virtual disks. The volume force varies in the radial direction, with the radial distribution of the force components based on the optimal distribution of Goldstein implemented as described by Stern, Kim, and Patel.[10] The thrust and power are interpolated from experimental values of the uninstalled propeller in axial flow, with the implicit assumption that these values do not change substantially when the propellers are operated in front of the wing and that the propeller normal force is negligible at the angles of attack of interest.

C. RANS: FUN3D

In addition to the STAR-CCM+ analysis, steady-state RANS simulation were performed with FUN3D, a node-centered, unstructured-grid, upwind-based RANS code.[11] These simulations employ the same source geometry as the STAR-CCM+ simulations, although the mesh geometries differ. The turbulence model used is the Spalart-Allmaras one-equation model with rotation/curvature correction and a quadratic constitutive relation turbulent diffusion model;[12] these simulations were limited to fully turbulent flow. The propellers are modeled by actuator disks, using the same formulation as the STAR-CCM+ analysis.

D. Results

Figure 2 shows exemplary pressure coefficient contours from a STAR-CCM+ solution. Figure 3 compares results with different solvers and turbulence models. Note from figure 3(d) that the agreement between VSPAERO and STAR-CCM+ is better on the wing only than on the combined wing and flap results shown in figure 3(c); this is presumably due to the inability of VSPAERO to model the performance of the stalled flap section as accurately.

Unless otherwise noted, the results shown are STAR-CCM+ solutions using the SST k-ω turbulence model of the blown wing with 40° flaps at the design conditions of 61.0 knots calibrated airspeed at 2,300 ft MSL and 60°F. Pitching moments are calculated about the wing root quarter-chord.

IV. Experimental Analysis

Full-scale testing was performed by constructing the wing, nacelles, and propellers with carbon fiber and mounting them to a support structure on a specially-modified truck such that the quarter-chord is 20 feet above the ground (see figure 4). The propellers are powered by Joby JM1 motors. This test apparatus is named Hybrid Electric Integrated Systems Testbed (HEIST). The most significant differences between the HEIST configuration and the idealized computational analysis models are:

- the ground plane (providing a small ground effect)
- the flap brackets

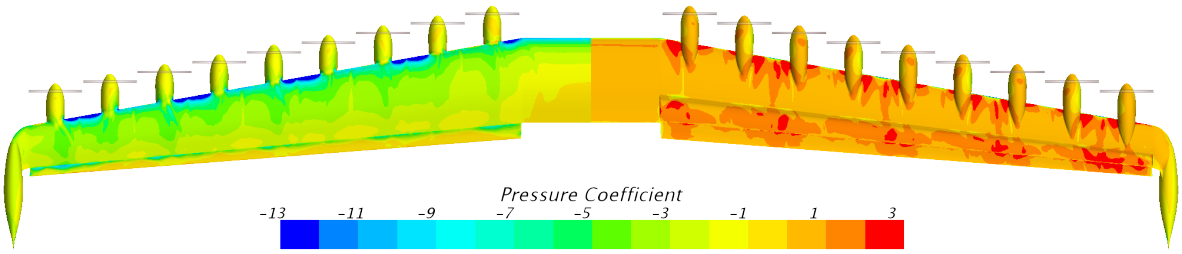

Figure 2. Pressure coefficient contours on the upper and lower surface from STAR-CCM+ results at $\alpha = 9°$

- the wing support structure
- the propeller spinners, which were not used on HEIST for simplicity

In addition, although the HEIST nacelles are sized for custom motor controllers, time and budget constraints prevented development of these controllers. Instead, larger COTS motor controllers (the MGM COMPRO HBC 280120), which partially protrude from the the nacelles, are used. The ground, truck, support structure, and motor controller geometries were all analyzed with limited STAR-CCM+ simulations to confirm that ignoring these differences will not significantly skew the computational results (see figure 6).

The steel wing support structure is suspended on the truck frame with airbags, to isolate the support structure from road vibrations. Large water tanks are mounted to this structure below the airbags to lower the center of mass of this suspended structure. The wing can be mounted to the support structure at any incidence angle between 0°and 15°, inclusive, and the flaps can be mounted at 10°, 20°, 30°, or 40°.

A. Instrumentation

The HEIST instrumentation suite comprises:

- GPS, to measure ground speed
- Inclinometer, to dynamically measure the angle of incidence
- A custom force balance with seven load cells, mounted between the wing and the support structure, to measure vertical force, axial force, side force, and pitching moment (see figure 7)
- Air data probe to measure incidence, sideslip angles, and airspeed
- Three uniaxial, three bixial, and two triaxial accelerometers to measure structural dynamics
- Motor controller communication providing RPM of each motor and input power into each motor controller
- Five chordwise strip-a-tubing steady pressure sensor strips with a total of 120 pressure measurements
- Eight high-speed transient pressure transducers

B. Results

Although full-speed HEIST experimental data is not yet available, lower-speed test data from the force balance is available and provides useful insight into the system performance. Figure 8 compares these results to STAR-CCM+ simulations at lower speeds. While the STAR-CCM+ results shown are at $C_{L_{\max}}$, the experimental results may be at a different angle of incidence. (The exact angle of incidence from these tests is not known, due to the lack of reliable inclinometer data at this point in the HEIST development.)

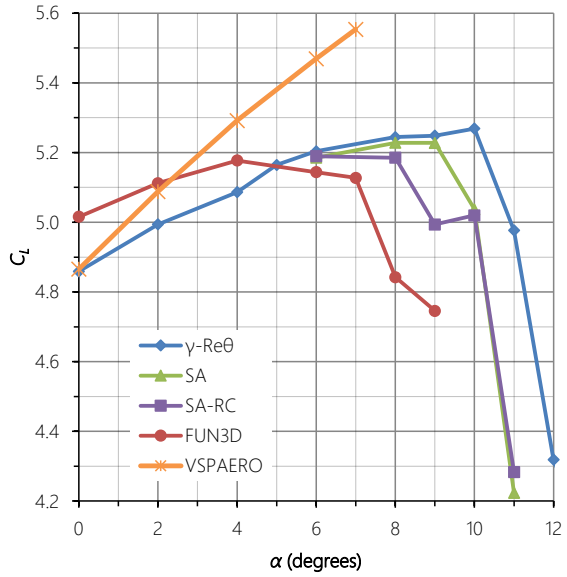

(a) Comparison of various STAR-CCM+ turbulence models with FUN3D results

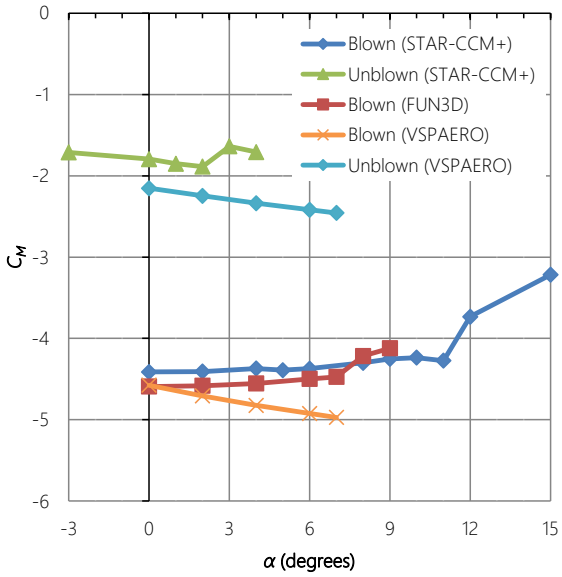

(b) Comparison of STAR-CCM+ and FUN3D pitching moment coefficients

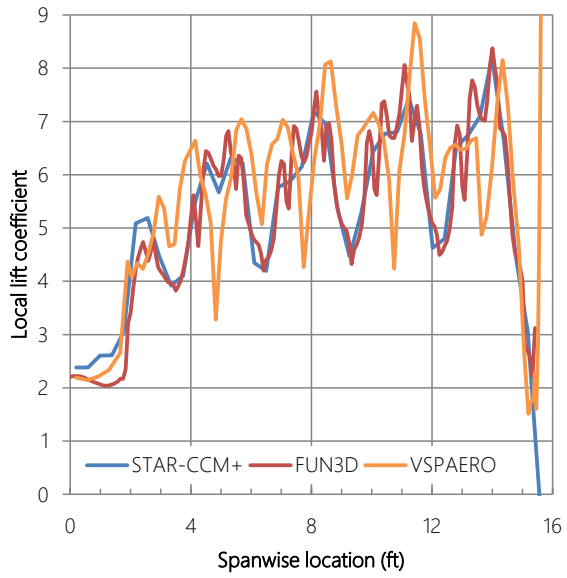

(c) Comparison of computational spanwise lift coefficient distribution at $\alpha = 6°$. The STAR-CCM+ data is smoother because it is calculated by summing the forces in spanwise bins, while the FUN3D and VSPAERO data shows lift coefficients at a series of spanwise sections.

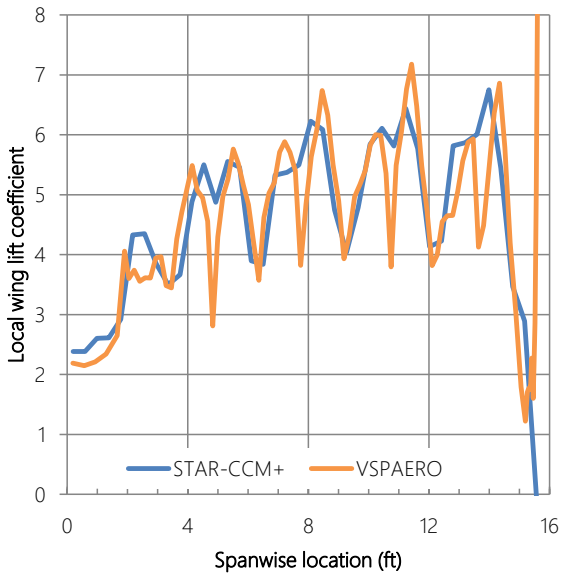

(d) Comparison of STAR-CCM+ and VSPAERO spanwise lift coefficient distribution from the wing only (excluding the flap) at $\alpha = 6°$.

Figure 3. Computational results

Figure 4. HEIST at NASA Armstrong (NASA photo)

Figure 5. The underside of the HEIST wing; the flap brackets as well as the motor controllers protruding from the lower nacelle surfaces are visible. The spinners are absent. The force balance is visible at the connection between the wing and the support structure.

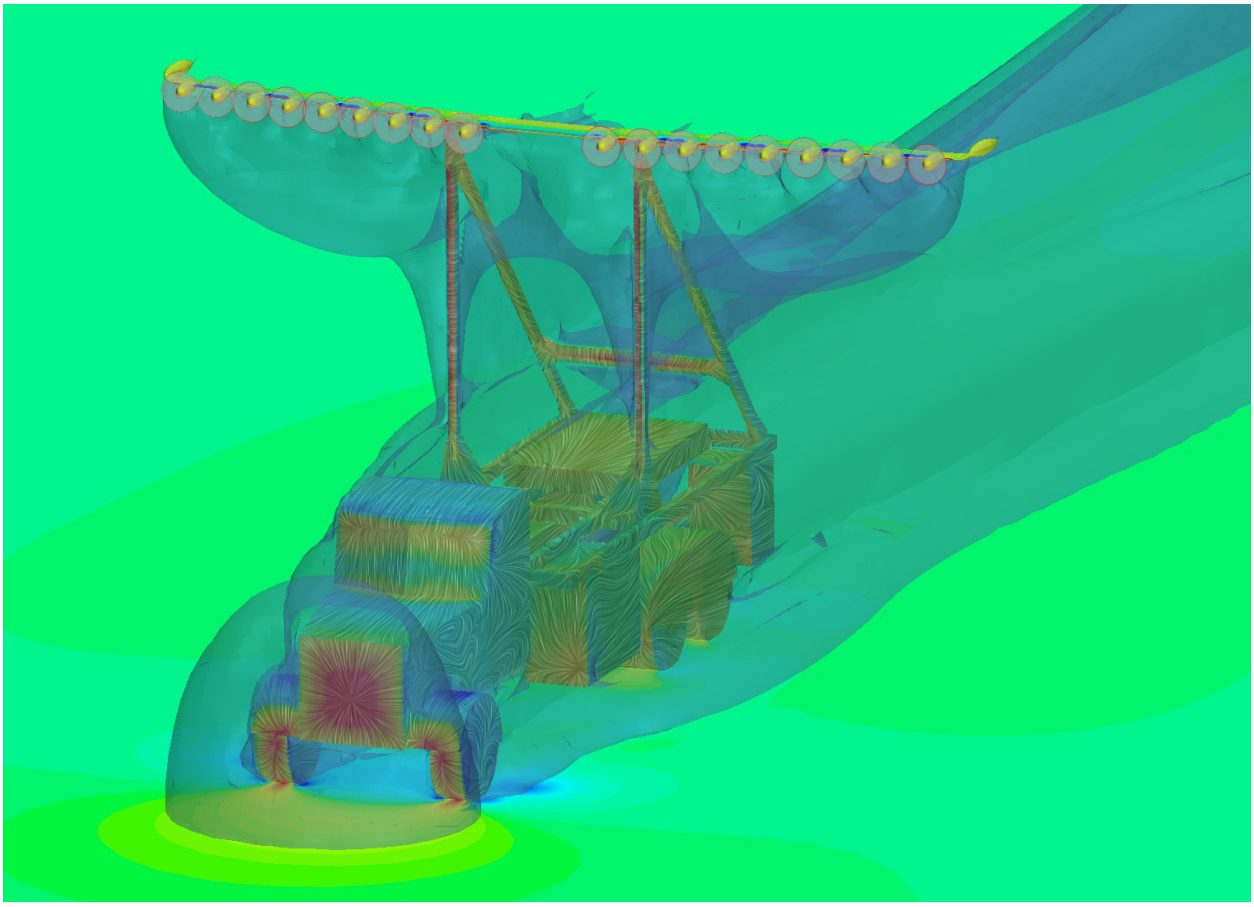

Figure 6. Example STAR-CCM+ analysis of the wing including the truck, support structure, and ground plane, showing pressure contours on the truck, wing, and ground (at different scales), with a isosurface of constant velocity magnitude to visualize the wake

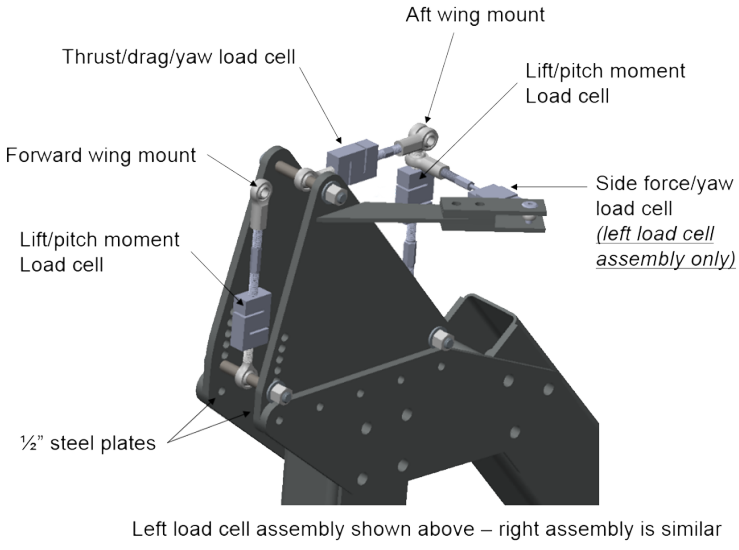

Figure 7. The load cell assembly

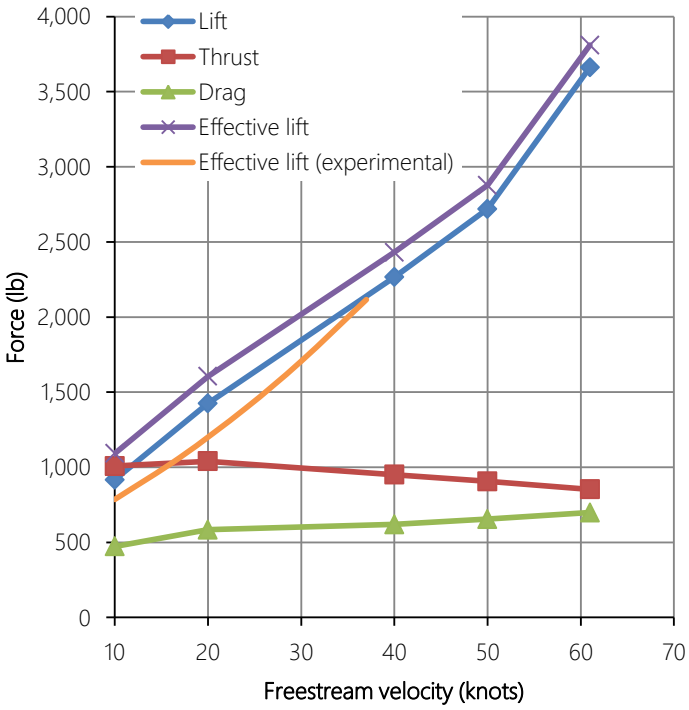

Figure 8. Comparison of STAR-CCM+ results with low-speed experimental results. "Effective lift" includes the vertical component of the propeller thrust. The experimental results curve shown is an average of quadratic fits to data from two runs in opposite directions.

V. Conclusion

Although only limited experimental data is available at the time of writing, the results are very promising. At the closest speed to the design speed at which experimental data is available, the analytical results differ from experimental results by about 10%, which is reasonably close considering the simplifying assumptions made in the simulations (namely modeling the propellers as steady actuator disks instead of fully-resolved unsteady rotating blades) and the uncertainty in these preliminary experimental results. More importantly, these results suggest that the performance at the design conditions of 61.0 knots calibrated airspeed will be reasonably close to the analytical predictions and will exceed the desired design $C_{L_{\max}}$ of 4.3, indicating that this configuration may be a viable path to lower cruise drag and improved ride quality.

Acknowledgments

The author would like to thank Joby Aviation, NASA, and Mark D. Moore for their support and mentorship through the course of this project. This research was funded by NASA Langley Research Center in support of its efforts to pursue understanding of the opportunities provided through highly coupled multidisciplinary integration of distributed electric propulsion. This research involved a close collaboration across NASA Langley, Armstrong, and Ames, with participation from a broad group of researchers. The author would like to extend appreciation to Dr. David Kinney, who provided the VSPAERO analysis; Karen Deere and Sally Viken, who provided the FUN3D analysis; Mike Park, who implemented the actuator disk model in FUN3D; Empirical Systems Aerospace, Inc., who spearheaded the instrumentation design, integration, and testing of HEIST; William Langford, who extensively analyzed the structure and dynamics of HEIST; and Sean Clarke and Starr Ginn, who oversaw the experimental and execution aspects of the program, acted as liaisons with NASA, provided additional resources, and provided test data.

References

[1]Stoll, A. M., Bevirt, J., Moore, M. D., Fredericks, W. J., and Borer, N. K., "Drag Reduction Through Distributed Electric Propulsion," *14th AIAA Aviation Technology, Integration, and Operations Conference*, American Institute of Aeronautics and Astronautics, June 2014.

[2]Conway, J. T., "Analytical solutions for the actuator disk with variable radial distribution of load," *Journal of Fluid Mechanics*, Vol. 297, 1995, pp. 327–355.

[3]Johnson, W., *Helicopter Theory*, Dover Publications, Inc., 1980.

[4]Menter, F. R., "Two-Equation Eddy-Viscosity Turbulence Models for Engineering Applications," *AIAA Journal*, Vol. 32, No. 8, 1994, pp. 1598–1605.

[5]Durbin, P., "On the k-3 stagnation point anomaly," *International Journal of Heat and Fluid Flow*, Vol. 17, No. 1, 1996, pp. 89–90.

[6]Langtry, R. B., *A Correlation-Based Transition Model using Local Variables for Unstructured Parallelized CFD codes*, Doctoral thesis, University of Stuttgart, 2006.

[7]Menter, F. R., Langtry, R., Likki, S., Suzen, Y., Huang, P., and Völker, S., "A Correlation-Based Transition Model Using Local Variables - Part I: Model Formulation," *Journal of Turbomachinery*, Vol. 128, No. 3, 2006, pp. 413–422.

[8]Spalart, P. R. and Allmaras, S. R., "A One-Equation Turbulence Model for Aerodynamic Flows," 1992.

[9]Shur, M. L., Strelets, M. K., Travin, A. K., and Spalart, P. R., "Turbulence modeling in rotating and curved channels: Assessing the Spalart-Shur correction," *AIAA Journal*, Vol. 38, No. 5, 2000, pp. 784–792.

[10]Stern, F., Kim, H., Patel, V., and Chen, H., "A viscous-flow approach to the computation of propeller-hull interaction," *Journal of Ship Research*, Vol. 32, No. 4, 1988, pp. 246–262.

[11]Anderson, W. K. and Bonhaus, D. L., "An Implicit Upwind Algorithm for Computing Turbulent Flows on Unstructured Grids," *Computers & Fluids*, Vol. 23, No. 1, 1994, pp. 1–21.

[12]Mani, M., Babcock, D., Winkler, C., and Spalart, P., "Predictions of a supersonic turbulent flow in a square duct," *AIAA Paper*, Vol. 860, 2013, pp. 2013.